High-pressure Raman response of single-walled carbon nanotubes: Effect of the excitation laser energy

Ahmad J. Ghandour,* David J. Dunstan, and Andrei Sapelkin
Department of Physics, Queen Mary University of London, Mile End Road, London El 4NS, United Kingdom

John E. Proctor
Center for Science at Extreme Conditions, University of Edinburgh, Mayfield Road, Edinburgh EH9 3JZ, United Kingdom

Matthew P. Halsall
School of Electronic Engineering, University of Manchester, Sackville Street, Manchester M60 1QD, United Kingdom
(Received 5 June 2008; revised manuscript received 21 July 2008; published 29 September 2008)

We report high-pressure Raman experiments on the tangential vibrational modes of CarboLex bundled single-walled carbon nanotubes up to 6.5 GPa using two different excitation energies: 1.96 and 2.41 eV. We show through the curve-fitting technique, together with the modified interband transition energies versus diameter plot, how the nature of the resonant tubes is modified under the excitation energy, in particular under the 1.96 eV excitation. Having metallic and semiconducting tubes in resonance at ambient pressure, we find that only semiconducting tubes are in resonance at 3.5 GPa. We associate this loss of resonance from the metallic tubes to a redshift pressure response of the first (E_{11}) transition energies from these tubes. Added to that, the change in the excitation energies leads to a change in the value of the transition pressure. This is simply associated with the fact of having different diameters in resonance under each excitation from the same sample.

DOI: 10.1103/PhysRevB.78.125420 PACS number(s): 78.30.Na, 61.46.Fg, 62.50.−p, 78.67.Ch

I. INTRODUCTION

Since their discovery in 1991,[1] single-walled nanotubes (SWNTs) have been of increasing scientific and technological interest due to their unusual physical properties resulting from their one-dimensional structure, which results in outstanding electronic and physical properties.

Recently theoretical[2–7] and experimental[8–13] studies have shown high pressure to be a very useful tool for investigating the influence of radial deformation and collapse of the tubes on their mechanical and electronic/optical properties.

Ab initio[2,3] calculations and molecular-dynamics (MD) simulations[4–6] on individual[4,6] and bundled[5] models of SWNTs predict a circular to oval structural transition at a transition pressure $P_t \sim 1/d^3$, where d is the nanotube diameter.[4,6] Using *ab initio* methods, Reich *et al.*[3] found that the transition pressure for tubes with a diameter of 0.8 nm would be in the interval 9–15 GPa. While, using molecular-dynamics simulations, Sun *et al.*[4] found the transition to be in the range of 1–5 GPa for HiPco SWNTs (diameter range of 1.3–0.8 nm).

High-pressure experiments on bundled SWNTs[8–11] revealed a wide range of results. Venkateswaran *et al.*[8] and Peters *et al.*[9] reported that for purified SWNTs with $d_t \sim 1.35$ nm there is a disappearance of the radial breathing mode (RM) and a significant decrease in the intensity of the tangential mode (GM) in the range of 1.5–2 GPa; this was attributed to a decrease in the cylindrical symmetry of the tubes to a hexagonally distorted cross section under compression. In contrast, Teredesai *et al.*[10,11] using 1.25–1.4 nm SWNTs, reported a uniform blueshift of the peaks up to 10 GPa with no significant changes in the intensity of the GM. However, they recorded a redshift of the GM over the range of 10–16 GPa, followed by another blueshift. They concluded that the hexagonal distortion is taking place at higher-pressure range (10–16 GPa) than was predicted (1.5–2 GPa).[8,9]

A remarkable aspect while performing high-pressure Raman spectroscopy on nanotubes is the sensitivity of the electronic structure of these tubes to pressure. Theoretical[7] and experimental[12,13] studies have shown variations in the values of the interband transitions from semiconducting tubes (E_{ii}^s) under high pressure.

According to the *ab initio* calculations of Okada *et al.*[7] a radial distortion in the nanotubes will modify the interband transition energies of these tubes (E_{ii}), hence taking some tubes been in resonance with the excitation energy at ambient pressure to be out of resonance and vice versa. In most cases, the pressure dependence is found to be negative, leading to a general decrease in the resonance energies. In their high-pressure absorption study on dispersed HiPco nanotube, Wu *et al.*[12] reported a redshift response from the first (E_{11}) and second (E_{22}) transition energies of the semiconducting nanotubes with a rate of up to −46 and −16 meV/GPa, respectively. On the other hand, Lebedkin *et al.*,[13] through a photoluminescence (PL) experiment, observed large downshifts of up to −80 meV/GPa for both E_{11}^S and E_{22}^S energies when probing SWNTs in sodium dodecyl sulphate (SDS) dispersion under pressure of up to 1 GPa. Notice that all the experimental studies on the pressure induced shift of the interband transition energies of SWNTs exposed results on semiconducting nanotubes, while up to date nothing could be found regarding transition energies from the metallic tubes. This is due to a lack in the experimental techniques, such, for example, metallic nanotubes are nonluminescent, and hence we cannot apply PL experiments on these tubes.

In this paper, we suggest that the interband transitions in the metallic tubes will have a nonzero response to the applied pressure. This is due to a loss of resonance from these tubes at 3.5 GPa. Such a loss have not been reported before for the presented experimental conditions. Hence, following that, a detailed analysis from the plot of the transition energies versus the tube diameter will suggest a redshift response from these energies. On the other hand we estimate the value of the transition pressure under different excitation energies and found that this pressure will vary with the excitation energy. This is simply due the resonance phenomena, i.e., different excitations are in resonance with different (n,m) tubes, hence different diameters. This is in good agreement with the previous predictions $(P \sim 1/d^3)$.

II. EXPERIMENTS

Our sample is composed of as-produced CarboLex AP Grade nanotubes commercially available from Sigma-Aldrich. They are single-walled nanotubes grown by the arc method. They have a diameter range of 1.2–1.5 nm and they are found in bundles of approximately 20 μm in length. The purity is 50%–70% with catalyst impurities consisting of Ni and Y nanoparticles encapsulated in carbon shells and small amounts of amorphous carbon (information supplied by manufacturer[14]).

All Raman spectra were recorded at room temperature using Renishaw instruments. Both 632.8-nm (1.96 eV) He-Ne and 514-nm (2.41 eV) Argon laser lines were used. The high-pressure Raman measurements were performed in a standard miniature-cryogenic diamond anvil cell (MCDAC) for the higher-pressure range and a MCDAC in the Zen configuration[15] was used for better control in the lower-pressure range. The lower-energy mode $\sim$200 cm^{-1} (radial breathing mode) could not be reliably collected under the 1.96 eV excitation due to specifics in the experimental setup (using of a holographic notch filter), while we have recorded this mode at ambient pressure under the 2.41 eV excitation. Therefore, we shall focus only on the high-energy first-order tangential Raman mode (GM), which occurs in the range 1500–1650 cm^{-1}. The hydrostatic pressure was measured using the R line emission of a small chip of ruby placed in the diamond anvil cell (DAC). This allows calibration of the pressure to within $\pm$0.1 GPa.[16] Solid SWNT materials were loaded directly into the DAC and pure ethanol was used as the pressure transmitting medium as it could be easily loaded, and it solidifies around 9 GPa, hence providing a good hydrostatic medium in our pressure region (0–6.5 GPa). Static scans were centered at 1600 cm^{-1} and the integration time was varied between 50 and 500 s depending on the strength of the Raman signal.

The set of experiments using the 1.96 eV excitation was recorded at Queen Mary University of London, while the one using the 2.41 eV laser was recorded at Manchester University.

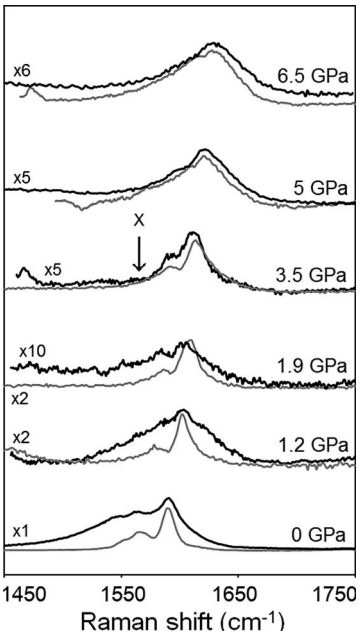

FIG. 1. GM spectra under pressure from the two set of experiments using 1.96 ($G^{1.96}$ in black) and 2.41 eV ($G^{2.41}$ in gray) excitation energies. The positions of the most intense bands in each spectrum are marked at different pressures. A blueshift is observed with increasing pressure for all the bands of the two spectra ($G^{1.96}$ and $G^{2.41}$). At 1.9 GPa the intensity of the $G^{1.96}$ spectrum is collapsed. At 3.5 GPa, the intensity of the $G^{1.96}$ spectrum is recovered, however a loss of the lower-frequency band is recorded (at the point marked "X"). At higher pressures, the bands in both spectra are broadened.

III. RESULTS

Figure 1 presents the spectra of the GM from each set of experiments at various pressures, with the black and gray spectra ($G^{1.96}$ and $G^{2.41}$) obtained using the 1.96 and 2.41 eV laser energies, respectively. At lower pressure, we can easily identify three bands in the $G^{1.96}$ spectra, in contrast to $G^{2.41}$ where there are only two main bands (as marked in Fig. 1). As pressure is increased, the bands of both spectra follow a blueshift with nearly the same rate of 8 ± 0.5 cm^{-1} GPa^{-1} (Fig. 2), and the scattering intensity is reduced. Transitions appear to take place at different pressures in the region 1.2–1.9 GPa leading to a marked break in the rate of shift of the bands and a drop in their intensity. This was particularly noticeable in the case of $G^{1.96}$, which shows a huge collapse in intensity around 1.9 GPa. The $G^{1.96}$ spectrum starts to recover at higher pressures up to 3.5 GPa where a full recovery relative to the $G^{2.41}$ spectrum is obtained. A change in the $G^{1.96}$ spectrum is also observed at this pressure (3.5 GPa) with the loss of the lower-frequency band (marked by "X" in Fig. 1). Above 3.5 GPa two bands are observed in both $G^{1.96}$ and $G^{2.41}$ spectra, broadened and blueshifted with the same new rate of 4.8 ± 0.4 cm^{-1} GPa^{-1} (Fig. 2) all the way up to 6.5 GPa.

As the spectra depend strongly on pressure, it was difficult to determine unambiguously the exact number of peaks necessary to fit each Raman spectrum. Consequently, the

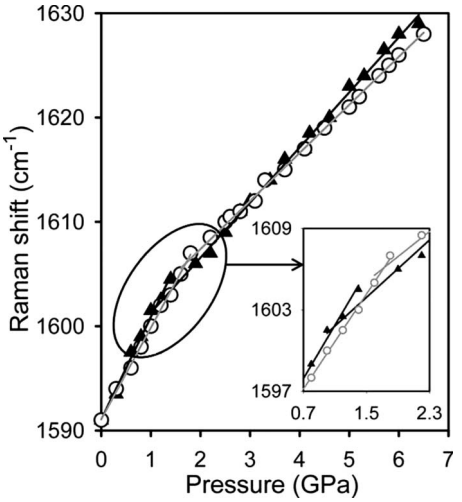

FIG. 2. Pressure evolution of the frequency of the most intense peak $G1$ from both sets of experiments using 1.96 (filled triangles) and 2.41 eV (open circles). The inset shows the transition region with the linear fits to the triangles (black lines) and the circles (gray lines) before and after transition. The intersection of each corresponding linear fits (black or gray) results in different transition pressures at 1.0 ± 0.1 GPa and 1.7 ± 0.1 GPa for $G^{1.96}$ and $G^{2.41}$, respectively.

unique feature that could be plotted with confidence was the position of the most intense peak $G1$, which is found to be at the same position at ambient pressure (~ 1590 cm^{-1}) in both $G^{1.96}$ and $G^{2.41}$ spectra. The shift of this peak with pressure recorded from each set of experiments is plotted in Fig. 2. The filled triangles and open circles represent the position of $G1$ in $G^{1.96}$ and $G^{2.41}$ spectra, respectively. Linear regression fitting suggests two linear fits for each data set, with different rates of shift. The experimental value for the pressure transition P_t, at which the rate of shift of both $G^{1.96}$ and $G^{2.41}$ decreases, is identified with the position of the point of intersection for the two lines corresponding to each set (triangles or circles). This is at 1.0 ± 0.1 GPa for $G^{1.96}$ and 1.7 ± 0.1 GPa for $G^{2.41}$ (inset in Fig. 2).

IV. DISCUSSION

Although most of our results have been reported and explained before, the enormous change in the profile of the $G^{1.96}$ spectrum at 3.5 GPa, to our knowledge, has yet not been observed. Moreover, the recorded difference in the value of the transition pressure from the same sample is still unclear.

A. Loss of the lower-frequency band

In order to understand the changes in the different GM spectra, from being different at 0 GPa into two similar spectra at 3.5 GPa, we will refer, at the first instant, to the curve fitting of these spectra. Notice that the significant changes leading to this behavior arises from the changes in the profile of the $G^{1.96}$ spectrum, while the profile of the $G^{2.41}$ follows the general usual behavior, which has been reported in many studies before (intensity decreases, broadening of the bands …). The changes in the $G^{1.96}$ spectrum, where mainly associated with the lower broadened bands.

Rao *et al.*[17] were the first to report the changes in the GM spectrum of SWNTs (recorded at ambient pressure) from having relatively sharp bands at low (<1.7 eV) and high (>2.2 eV) excitation energies (E_{Laser}) to broadened and downshifted bands for energies between 1.7–2.2 eV. Kataura *et al.*[18] and Alvarez *et al.*[19] fitted these broadened and downshifted band, of the GM spectrum collected in the range 1.7–2.2 eV, using an asymmetric Breit-Wigner-Fano (BWF) line shape. They referred to the presence of this peak as a confirmation of having metallic tubes in resonance. While the origin of this asymmetric peak was still controversial, Brown *et al.*[20] confirmed in their study the need for this BWF peak in order to account for the lower-frequency feature of the metallic tubes (~ 1540 cm^{-1}) in addition to a Lorentzian line shape ($G+$) to account for the higher-frequency feature (~ 1582 cm^{-1}) of the same tubes, hence resulting in only two peaks to fit the entire GM of metallic tubes. Knowing that the difference in the frequencies of the upper features and lower features of the GM for all the tubes been associated to a difference in the force constant for vibrations along the tube axis (higher force constant) versus circumferentially (lower force constant), the additional downshifting and broadening of the lower-frequency peak (from the those seen at lower and higher energy) was attributed to the coupling of the discrete phonons to an electronic continuum, resulting in the BWF line shape.[20]

On the other hand, Jorio *et al.*[21] studied the spectra of semiconducting nanotubes through a polarized Raman experiment. They found that the GM of these tubes is composed of four Lorentzian peaks, $G1$ at 1590 cm^{-1}, $G2$ at 1567 cm^{-1}, $G3$ at 1549 cm^{-1}, and $G4$ at 1607 cm^{-1}. The positions of these peaks, in particular the last three, could be modified due to curvature[21,22] or chirality effects.[21,23]

Based on the findings of Brown *et al.*[20] and Jorio *et al.*,[21] we have performed a curve fitting (Fig. 3, left panel and right panel) for both GM spectra recorded at ambient pressure and at 3.5 GPa, respectively.

At ambient pressure, we found that the $G^{2.41}$ spectrum [Fig. 3(a), left panel gray] is well fitted using only the Lorentzians [Fig. 3(a), left panel black dotted] of Jorio *et al.* (with a small merged modification in their parameters), while for the $G^{1.96}$ spectrum [Fig. 3(b), left panel gray], we needed in addition to these Lorentzians [Fig. 3(b), left panel black dotted] the other two peaks of Brown *et al.*, the BWF, and the Lorentzian $G+$ at ~ 1580 cm^{-1} [Fig. 3(b), left panel solid black]. Notice that in the fitting of the $G^{1.96}$ spectrum, the relatively intense BWF peak will mask the relatively less intense $G3$ peak (centered in the same region). Hence, we deduce from both fittings that at ambient pressure the $G^{2.41}$ spectrum is a contribution of semiconducting SWNTs in resonance, in contrast to the $G^{1.96}$ spectrum, which has contributions from both semiconducting and metallic nanotubes in resonance.

On the other hand at 3.5 GPa, a good fit for the $G^{2.41}$ spectrum [Fig. 3(a), right panel gray) could be attained using three of the Lorentzians of Jorio *et al.* in particular, $G1$, $G2$, and $G4$, after taking into consideration the blueshift and the

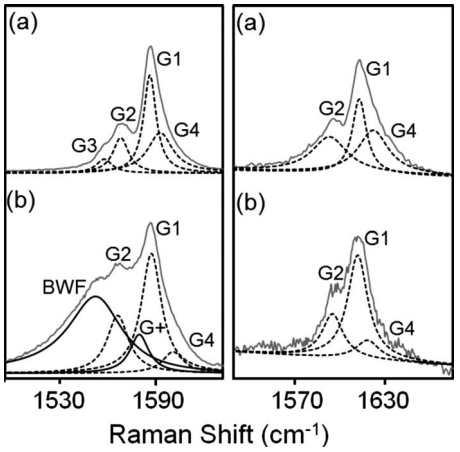

FIG. 3. Left panel: GM spectra (gray) recorded at ambient pressure under each excitation. (a) The $G^{2.41}$ spectrum is fitted using four Lorentzian peaks (black dotted). These peaks are associated with semiconducting tubes in resonance. (b) The $G^{1.96}$ spectrum is fitted using four Lorentzian peaks and a BWF line shape. Both the BWF peak ~1540 cm^{-1} and the Lorentzian "*G*+" ~1580 cm^{-1} (solid black) are a contribution of metallic tubes in resonance, while the other three Lorentzians (black dotted) are associated with the semiconducting tubes in resonance. Right panel: GM spectra (gray) recorded at 3.5 GPa under each excitation. (a) The $G^{2.41}$ spectrum fitted using three Lorentzians (black dotted: *G*1, *G*2, and *G*4 been shifted under pressure). This spectrum is still considered as a contribution of semiconducting tubes in resonance. (b) The $G^{1.96}$ spectrum fitted using only three Lorentzians (black dotted: *G*1, *G*2, and *G*4 have been shifted under pressure). As these Lorentzians are associated with semiconducting tubes in resonance, the absence of the BWF peak together with the *G*+ Lorentzian is associated to a loss of resonance from the metallic tubes.

broadening of these peaks [Fig. 3(a), right panel, black dotted). Taking into consideration that "*G*3" could be disappeared under the noise after a progressive decrease in its relatively low intensity, we associate this mode once again to semiconducting tubes in resonance. However, the similar $G^{1.96}$ spectrum at this pressure [Fig. 3(b), right panel, gray] is well fitted also using the same peaks [Fig. 3(b), right panel, black dotted] as those used for the corresponding $G^{2.41}$ with a small modification in their center and width, and hence also semiconducting nanotubes are in resonance with the 1.96 eV excitation at this pressure. But as a good fit was attained using only these three Lorentzians (*G*1, *G*2, and *G*4), the no need for the BWF peak and the other Lorentzian *G*+, or in other words the disappearance of these peaks, could be attributed to many different reasons.

Paillet *et al.*[24] have seen the disappearance of the BWF peak, but this was only upon transforming from bundled to isolated metallic SWNTs, and hence as we are using bundled tubes with ethanol as pressure transmitting media, there is no possibility for such isolation.

On the other hand, Christofilos *et al.*,[25] using Raman spectroscopy, also studied the pressure response of both bundled single-wall and double-wall carbon nanotubes. They have just observed a progressive narrowing of the BWF peak, compounded with intensity attenuation, but not a sudden disappearance of the peak. They attributed this to a decoupling process, possibly connected to the enhanced tube-tube interaction and the deformation of the tubes at elevated pressures. Added to that, Merlen *et al.*[26] studies on single-walled carbon nanotubes, again, did not reveal any sudden disappearance; instead, they reported a progressive decrease in the relative intensity up to 20 GPa.

Here we suggest that the reason for this disappearance could be a loss of resonance from the contributing resonant tubes, the metallic tubes. Such a loss could be a result of a possible redshift in the interband transition energies of these tubes.

1. Redshift of the transition energies

Resonance Raman spectra of SWNTs can be strongly affected by shifts of optical transitions under pressure. In most cases, this shift was found to be negative[12,13] leading to a general decrease in the resonance energies. Although all of the experimental studies have been concerned with transitions from semiconducting tubes, and as nothing could be found for transitions in metallic tubes, hereby we put an assumption that the interband transitions from metallic tube will have a nonzero pressure response, and then we deduce that this response is of negative value.

A plot for all the possible interband transition energies (E_{ii}) from the tubes of the used sample in the region of both excitation energies and at ambient pressure is presented in Fig. 4(a). This plot was generated using the data of Araujo *et al.*[27] for the interband transitions in unbundled SWNTs after applying the corrections of Rao *et al.*[28] and O'Connell *et al.*[29] in order to account for bundled metallic and semiconducting tubes (unbundled to bundled → blueshift of E_{ii}^{M} and redshift of E_{ii}^{S}), respectively.

Although the sample diameter range is 1.2–1.5 nm (as supplied by manufacturer[14]), the RM collected at ambient pressure under the 2.41 eV excitation (Fig. 5) have shown the presence of two peaks centered at 150 and 175 cm^{-1}. This implies the presence of some resonant tubes with a diameter ~1.6 nm (applying $\omega_{RBM}=150$ cm^{-1} in $\omega_{RBM}=217.8/d_t+15.7$)[27] in our sample.

Based on this, Fig. 4 was plotted with the diameter range of 1.2–1.6 nm and not 1.2–1.5 nm.

The window bounded by the two dotted black lines and centered at 1.96 eV represents the resonance window of the semiconducting tubes as averaged by O'Connell *et al.*[29] (average resonance width for semiconducting tubes is ~50 meV). We have averaged this also for the metallic tubes. The same applies for the window bounded by the dotted gray lines and centered at 2.41 eV. Following that, we can see that at ambient pressure [Fig. 4(a)] both metallic and semiconducting tubes are in resonance within the 1.96 eV excitation, while only semiconducting tubes are in resonance with the 2.41 eV excitation.

While applying pressure, the transitions from semiconducting tubes will follow a redshift, as predicted,[12,13] hence taking more tubes into resonance with the 1.96 eV excitation, while some changes in the resonant tube diameters were to occur under the 2.41 eV excitation but no changes in the nature of these tubes (semiconducting are still in resonance). On the other hand, from Fig. 4(a), we can see that most of

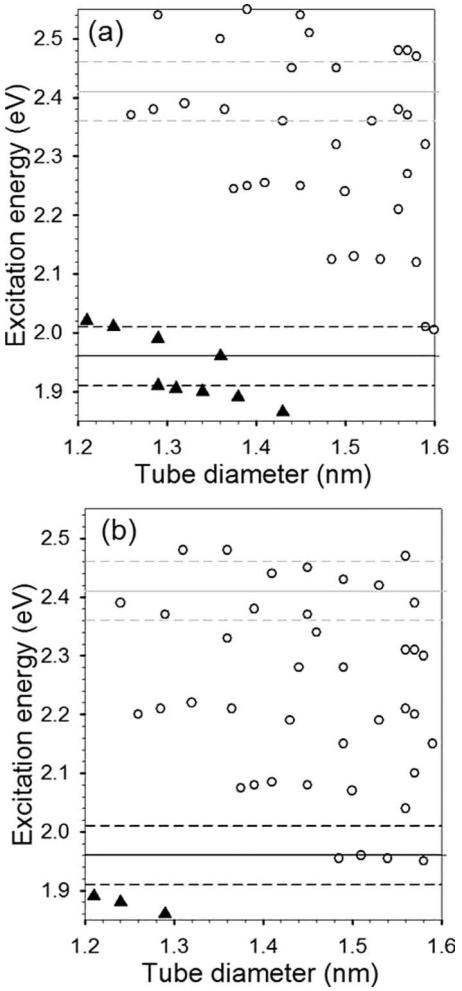

FIG. 4. Optical interband transition energies (E_{ii}) versus tube diameters (d_t) for all the tubes in the diameter range of the used sample (a) at ambient pressure and (b) at 3.5 GPa. The two solid lines (black and gray) represent the laser excitation energies (1.96 and 2.41 eV, respectively), while the two dotted lines (black or gray), represent the resonance window within each of the excitation energies (1.96 or 2.41 eV, respectively). Filled triangles refer to "E_{11}" from metallic tubes, while open circles to "E_{33}" and "E_{44}" from semiconducting tubes. All data have been plotted at ambient pressure using Refs. 27–29, while we suggest a redshift of ~35 meV/GPa for plot "*b*."Based on the proposed shift, all "E_{11}" from metallic tubes will be out of the resonance window, hence no resonance from metallic tubes is expected.

the transitions associated with metallic tubes (triangles) are presented either between or below the boundaries of the 1.96 eV resonance window, while just few of these transitions are presented above the upper boundary of this window. Based on that, we can deduce that a possible loss of resonance from metallic tubes would only occur if these transitions, in general, obey a redshift under pressure, hence graphically taking all the symbols presented in and above the resonance window to shift down and attain a values less than the lower dotted black boundary line of this window (~1.91 eV). Assuming this is what is happening, then we suggest from our results that the minimum pressure needed for such a loss will be 3.5 GPa. For more clarity, we plot all of these results in Fig. 4(b). Hence this plot presents all the interband transitions from the sample tubes in the region of the excitation energies at 3.5 GPa.

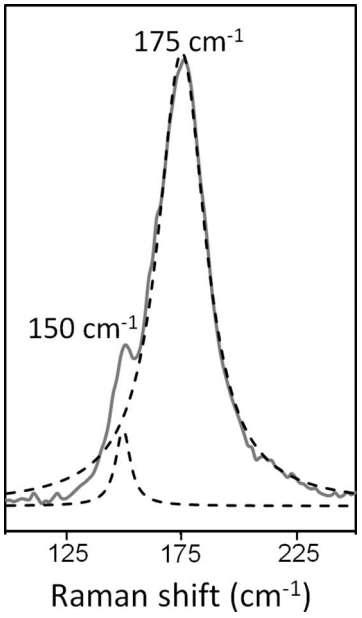

FIG. 5. RM collected using the 2.41 eV excitation at ambient pressure. Two clear peaks are presented at 150 and 175 cm^{-1}. According to Araujo *et al.* (Ref. 27), these peaks correspond to resonance from tubes centered ~1.6 and 1.4 nm, respectively, with the high contribution from those of ~1.4 nm.

B. Transition pressure

Now we move on to the second minor result in our study, the difference between the recorded transition pressure values.

As we have estimated the values of the transition pressures from the pressure response of the most intense peak "*G*1" (plotted from both $G^{1.96}$ and $G^{2.41}$), it is important at the first instance to understand the origin of this peak in the two different spectra.

Although we have some difference in the nature of the resonant tubes under each excitation, *G*1, which was found from both to be centered ~1590 cm^{-1}, is a contribution of only semiconducting nanotubes in resonance within each excitation.

From Fig. 4(a) we can see that the semiconducting tubes within the resonance window of the 1.96 eV excitation are centered nearly ~1.6 nm, while a wide diameter range of semiconducting tubes are in resonance with the 2.41 eV excitation. But as the most intense peak in the collected RM (Fig. 5) is centered ~175 cm^{-1}, then the GM collected under the 2.41 eV excitation is mainly a contribution of the tubes centered ~1.4 nm (ω_{RBM}=175 cm^{-1}). Hence, the 1590 cm^{-1} peak in the $G^{2.41}$ and $G^{1.96}$ spectra comes from semiconducting tubes of diameters 1.4 and 1.6 nm, respectively. Adding this result to the fact that the transition pressure is inversely proportional to the tube diameter,[4,6] we deduce a ratio of "1:1.6" for the transition pressure under the different excitations, in agreement with our reported results

(1:1.7). Therefore we deduce that it is essential to know the exact diameter value of the resonant tubes not the mean diameter of the sample.

V. CONCLUSION

In summary, we have examined the GM spectra from one sample of SWNTs under pressure using two excitation laser energies. We relate the observed difference in the values of the transition pressure to the difference in the diameters of semiconducting tubes that are in resonance with each excitation energy. In addition, we observe changes in the profiles' shapes under pressure. These changes were associated with changes in the electronic nature of the resonant tubes. We associate these changes to a redshift in the transition energies of metallic nanotubes (E_{11}). As the literature reports few studies of such energy shifts from metallic nanotubes, further studies are required to understand this phenomenon.

ACKNOWLEDGMENTS

One of the authors (A.J.G.) thanks the Al Tajir Trust for financial support.

*ghandour_ahmad@hotmail.com

[1] S. Iijima, Nature (London) **354**, 56 (1991).
[2] S.-P. Chan, W.-L. Yim, X. G. Gong, and Z.-F. Liu, Phys. Rev. B **68**, 075404 (2003).
[3] S. Reich, C. Thomsen, and P. Ordejon, Phys. Status Solidi B **235**, 354 (2003).
[4] D. Y. Sun, D. J. Shu, M. Ji, Feng Liu, M. Wang, and X. G. Gong, Phys. Rev. B **70**, 165417 (2004).
[5] X. H. Zhang, D. Y. Sun, Z. F. Liu, and X. G. Gong, Phys. Rev. B **70**, 035422 (2004).
[6] P. Tangney, R. B. Capaz, C. D. Spataru, M. L. Cohen, and S. G. Louie, Nano Lett. **5**, 2268 (2005).
[7] S. Okada, A. Oshiyama, and S. Saito, J. Phys. Soc. Jpn. **70**, 2345 (2001).
[8] U. D. Venkateswaran, A. M. Rao, E. Richter, M. Menon, A. Rinzler, R. E. Smalley, and P. C. Eklund, Phys. Rev. B **59**, 10928 (1999).
[9] M. J. Peters, L. E. McNeil, J. P. Lu, and D. Kahn, Phys. Rev. B **61**, 5939 (2000).
[10] P. Teredesai, A. Sood, D. Muthu, R. Sen, A. Govindaraj, and C. Rao, Chem. Phys. Lett. **319**, 296 (2000).
[11] P. V. Teredesai, A. K. Sood, S. M. Sharma, S. Karmakar, S. K. Sikka, A. Govindaraj, and C. N. R. Rao, Phys. Status Solidi B **223**, 479 (2001).
[12] J. Wu, W. Walukiewicz, W. Shan, E. Bourret-Courchesne, J. W. Ager, K. M. Yu, E. E. Haller, K. Kissell, S. M. Bachilo, R. B. Weisman, and R. E. Smalley, Phys. Rev. Lett. **93**, 017404 (2004).
[13] S. Lebedkin, K. Arnold, O. Kiowski, F. Hennrich, and M. M. Kappes, in *Electronic Properties of Novel Nanostructures*, AIP Conf. Proc. No. 786 (AIP, Melville, NY, 2005), pp. 124–128.
[14] www.sigmaaldrich.com
[15] N. W. A. Van Uden and D. J. Dunstan, Rev. Sci. Instrum. **71**, 4174 (2000).
[16] G. J. Piermarini, S. Block, and J. D. Barnett, J. Appl. Phys. **44**, 5377 (1973).
[17] A. M. Rao, E. Richter, S. Bandow, B. Chase, P. C. Eklund, K. W. Williams, M. Menon, K. R. Subbaswamy, A. Thess, R. E. Smalley, G. Dresselhaus, and M. S. Dresselhaus, Science **275**, 187 (1997).
[18] H. Kataura, Y. Kumazawa, Y. Maniwa, I. Umezu, S. Suzuki, Y. Ohtsuka, and Y. Achiba, Synth. Met. **103**, 2555 (1999).
[19] L. Alvarez, A. Righi, T. Guillard, S. Rols, E. Anglaret, D. Laplaze, and J.-L. Sauvajol, Chem. Phys. Lett. **316**, 186 (2000).
[20] S. D. M. Brown, A. Jorio, P. Corio, M. S. Dresselhaus, G. Dresselhaus, R. Saito, and K. Kneipp, Phys. Rev. B **63**, 155414 (2001).
[21] A. Jorio, G. Dresselhaus, M. S. Dresselhaus, M. Souza, M. S. S. Dantas, M. A. Pimenta, A. M. Rao, R. Saito, C. Liu, and H. M. Cheng, Phys. Rev. Lett. **85**, 2617 (2000).
[22] A. Jorio, A. G. Souza Filho, G. Dresselhaus, M. S. Dresselhaus, A. K. Swan, M. S. Unlu, B. Goldberg, M. A. Pimenta, J. H. Hafner, C. M. Lieber, and R. Saito, Phys. Rev. B **65**, 155412 (2002).
[23] D. Kahn and J. P. Lu, Phys. Rev. B **60**, 6535 (1999).
[24] M. Paillet, Ph. Poncharal, A. Zahab, J.-L. Sauvajol, J. C. Meyer, and S. Roth, Phys. Rev. Lett. **94**, 237401 (2005).
[25] D. Christofilos, J. Arvanitidis, C. Tzampazis, K. Papagelis, T. Takenobu, Y. Iwasa, H. Kataura, C. Lioutas, S. Ves, and G. A. Kourouklis, Diamond Relat. Mater. **15**, 1075 (2006).
[26] A. Merlen, N. Bendiab, P. Toulemonde, A. Aouizerat, A. San Miguel, J. L. Sauvajol, G. Montagnac, H. Cardon, and P. Petit, Phys. Rev. B **72**, 035409 (2005).
[27] P. T. Araujo, S. K. Doorn, S. Kilina, S. Tretiak, E. Einarsson, S. Maruyama, H. Chacham, M. A. Pimenta, and A. Jorio, Phys. Rev. Lett. **98**, 067401 (2007).
[28] A. M. Rao, J. Chen, E. Richter, U. Schlecht, P. C. Eklund, R. C. Haddon, U. D. Venkateswaran, Y.-K. Kwon, and D. Tománek, Phys. Rev. Lett. **86**, 3895 (2001).
[29] M. J. O'Connell, S. Sivaram, and S. K. Doorn, Phys. Rev. B **69**, 235415 (2004).